Delft University of Technology

Soft deposition of TCOs by pulsed laser for high-quality ultra-thin poly-Si passivating contacts

Ah Sen, Mike Tang Soo Kiong; Mewe, Agnes; Melskens, Jimmy; Bolding, Jons; van de Poll, Mike; Weeber, Arthur

DOI
10.1063/5.0158681

Publication date
2023

Document Version
Final published version

Published in
Journal of Applied Physics

Citation (APA)
Ah Sen, M. T. S. K., Mewe, A., Melskens, J., Bolding, J., van de Poll, M., & Weeber, A. (2023). Soft deposition of TCOs by pulsed laser for high-quality ultra-thin poly-Si passivating contacts. *Journal of Applied Physics*, *134*(15), Article 154502. https://doi.org/10.1063/5.0158681

Important note
To cite this publication, please use the final published version (if applicable).
Please check the document version above.

Copyright
Other than for strictly personal use, it is not permitted to download, forward or distribute the text or part of it, without the consent of the author(s) and/or copyright holder(s), unless the work is under an open content license such as Creative Commons.

Takedown policy
Please contact us and provide details if you believe this document breaches copyrights.
We will remove access to the work immediately and investigate your claim.

This work is downloaded from Delft University of Technology.
For technical reasons the number of authors shown on this cover page is limited to a maximum of 10.

Journal of Applied Physics

RESEARCH ARTICLE | OCTOBER 20 2023

Soft deposition of TCOs by pulsed laser for high-quality ultra-thin poly-Si passivating contacts

Mike Tang Soo Kiong Ah Sen ; Agnes Mewe ; Jimmy Melskens ; Jons Bolding ; Mike van de Poll ; Arthur Weeber

J. Appl. Phys. 134, 154502 (2023)
https://doi.org/10.1063/5.0158681

03 June 2024 13:21:40

Boost Your Optics and Photonics Measurements
Lock-in Amplifier
Zurich Instruments
Find out more
Boxcar Averager

Journal of Applied Physics ARTICLE pubs.aip.org/aip/jap

Soft deposition of TCOs by pulsed laser for high-quality ultra-thin poly-Si passivating contacts

Cite as: J. Appl. Phys. **134**, 154502 (2023); doi: 10.1063/5.0158681
Submitted: 17 May 2023 · Accepted: 1 October 2023 ·
Published Online: 20 October 2023

View Online

Export Citation

CrossMark

Mike Tang Soo Kiong Ah Sen,[1,2,a)] Agnes Mewe,[1] Jimmy Melskens,[1,3] Jons Bolding,[1,4] Mike van de Poll,[5] and Arthur Weeber[1,2]

AFFILIATIONS

[1]TNO Energy & Materials Transition Solar Energy, P.O. Box 15, NL-1755 ZG Petten, The Netherlands
[2]Delft University of Technology, PVMD group, Mekelweg 4, NL-2628 CD Delft, The Netherlands
[3]HyET Solar B.V., Westervoortsedijk 71K, 6827 AV Arnhem, The Netherlands
[4]Faculty of Science and Technology, University of Twente, AE 7500 Enschede, The Netherlands
[5]Department of Applied Physics, Eindhoven University of Technology, MB 5600 Eindhoven, The Netherlands

[a)]**Author to whom correspondence should be addressed:** m.t.s.k.ahsen@tudelft.nl

ABSTRACT

In this work, the applicability of pulsed laser deposition (PLD) of transparent conductive oxides (TCOs) on high-quality ultra-thin poly-Si based passivating contacts is explored. Parasitic absorption caused by poly-Si layers can be minimized by reducing the poly-Si layer thickness. However, TCO deposition on poly-Si contacts, commonly by sputtering, results in severe deposition-induced damage and further aggravates the surface passivation for thinner poly-Si layers (<20 nm). Although a thermal treatment at elevated temperature (~350 °C) can be used to partially repair the surface passivation quality, the contact resistivity severely increases due to the formation of a parasitic oxide layer at the poly-Si/ITO interface. Alternatively, we show that PLD TCOs can be used to mitigate the damage on ultra-thin (~10 nm) poly-Si layers. Further improvement in poly-Si contact passivation can be achieved by increasing the deposition pressure while low contact resistivities (~45 mΩ cm^2) and good thermal stability (up to 350 °C) are achieved with a PLD indium-doped tin oxide (ITO) layer on high-quality ultra-thin poly-Si(n^+) contacts. This allows for the application of a highly transparent front side contact by combining the excellent opto-electrical properties of a PLD ITO film with a 10 nm thin poly-Si contact.

03 June 2024 13:21:40

© 2023 Author(s). All article content, except where otherwise noted, is licensed under a Creative Commons Attribution (CC BY) license (http://creativecommons.org/licenses/by/4.0/). https://doi.org/10.1063/5.0158681

I. INTRODUCTION

Poly-Si passivating contacts have been extensively explored in recent years, enabling a record solar cell conversion efficiency of 26.4% in combination with a front side diffused emitter cell architecture.[1] This solar cell structure is limited by the front emitter recombination loss.[2] These recombination losses can be reduced by using a front and rear passivating contact approach, hence allowing for a better overall surface passivation quality. The drawback of poly-Si passivating contacts, when used at the front side of a solar cell, is the parasitic absorption caused by the high dopant concentration in the relatively thick contact materials. While the parasitic absorption losses can be mitigated by reducing the poly-Si layer thickness to below 20 nm, a transparent conductive oxide (TCO) layer is necessary to provide lateral conductivity for charge carrier transport to the metal grid. However, the subsequent deposition of a TCO film on poly-Si layers normally results in a drop in surface passivation properties of the cell.

TCOs are typically deposited by sputtering, which reduces the surface passivation quality of the contacts and has been generally reported for silicon heterojunction (SHJ) solar cells based on amorphous silicon layers.[3] Nevertheless, the sputtering-induced damage on SHJ solar cells can be recovered after low-temperature annealing treatment (~200 °C),[4] which is also an essential process to enable good contact between the TCO and screen-printed metal electrode. On the contrary, the sputtering-induced damage on poly-Si contacts is much more difficult to repair and requires a higher annealing temperature (>250 °C) in comparison with SHJ solar cells to reduce the deposition-induced damage.[5] This, in turn, impedes charge

© Author(s) 2023

carrier transport across the poly-Si/TCO interface possibly due to the formation of a SiO_x interfacial layer.[6–8] Additionally, ultra-thin poly-Si layers (<20 nm) suffer from more severe sputtering-induced damage, since they cannot properly shield the c-Si/SiO_x interface from UV radiation and/or particle bombardment.[9] Consequently, minimizing the poly-Si thickness to further improve the photogenerated current of the cell is compromised by the aggravating sputtering-induced surface passivation loss of the contact.

On the other hand, pulsed laser deposition (PLD) has demonstrated its "soft" deposition properties on sensitive layers in organic,[10,11] perovskite,[12] and, most recently, SHJ solar cells.[13] PLD is based on the ablation of a solid target by a focused UV laser beam with nanosecond pulses, resulting in the removal of the material from that target. This leads to the formation of a plasma plume that expands perpendicularly to the substrate, which results in the film growth. PLD has several unique characteristics that have been shown to be beneficial to control the growth of complex oxide thin films. For example, PLD allows for a vast range of tunability in processing parameters, since the laser source is physically decoupled from the processing chamber. Even though the physical aspects of PLD are relatively simple, the process deposition is intriguingly complex; the different process stages are often interrelated and overlap. Additionally, a large number of variable parameters exist and have direct influences on the layer properties.

In this work, we explore the influence of various PLD parameters on the optical and electrical properties of indium-doped tin oxide (ITO) and the impact of sputtering and PLD-induced damage of the surface passivation quality of ultra-thin poly-Si contacts. Additionally, the effect of a post-annealing treatment on the contact resistivity of our poly-Si contacts is investigated.

II. EXPERIMENTAL DETAILS

A. Sputtering and PLD of ITO layers

For comparison, a sputtered ITO film was deposited, as the reference, with an inline sputtering DC magnetron tool. An ITO target containing 90 wt. % of In_2O_3 and 10 wt. % of SnO_2 was used while the deposition was performed at room temperature (RT) with an O_2 flow of about 2.6 SCCM and a processing pressure of 0.01 mbar.

The PLD system, developed by Solmates BV, consists of a KrF excimer laser, which creates ultra-short laser pulses at a wavelength of 248 nm and is directed toward the ITO target (90/10 wt. % In_2O_3/SnO_2). The repetition rate and fluency of the laser correspond to the frequency and energy density of the laser, respectively. Additionally, the laser properties, chamber pressure, O_2 to Ar [Ar/(Ar + O_2)] partial pressure, and substrate temperature are varied, as shown in Table I. The samples were also subjected to post-deposition annealing treatment in air at temperatures ranging from 190 to 350 °C.

TABLE I. PLD ITO film parameters' variations.

PLD parameter	Values
Chamber pressure (mbar)	0.02–0.2
O_2/(Ar + O_2) ratio (−)	0.2–1
Substrate temperature (°C)	20–400
Repetition rate (Hz)	10–100
Laser fluence (J/cm^2)	0.93–1.55

B. ITO material characterization

Figure 1(a) shows the measurement schematic used to measure reflection and transmission of ITO films by using a Lambda 950 spectrophotometer. The carrier concentration (N_e) and mobility (μ_e) of the ITO films were determined by using Hall effect measurements on samples with a van der Pauw contact configuration. To perform such measurements, the ITO layer was deposited on a thick SiO_2 (∼450 nm) film, which was thermally grown on a polished crystalline silicon (c-Si) substrate. A spectroscopic ellipsometry measurement (SE) system (J.A. Woollam Co., Inc.) was utilized to determine the thickness (d), and the refractive index and absorption coefficient (n and k) of the films. Note that the backside of the Si substrate was intentionally left unpolished to minimize the contribution of backside reflection during SE measurement. Tauc–Lorentz and Drude oscillators were combined to model the optical parameters of our ITO films in both the ultraviolet and visible, and near infrared parts of the spectrum, respectively. The sheet resistance (R_{sheet}) was measured using the four-point probe technique, from which the layer resistivity (ρ) was determined according to $R_{sheet} = \rho/d$.

C. Processing and characterization of the passivating contacts

The impact of PLD ITO film deposition was investigated on a 20 nm thick poly-Si(n^+) contact. Figures 1(c) and 1(d) shows the symmetric passivation and contact resistance test structures, as well as the solar cell schematic, respectively. M2-sized Czochralski (Cz) n-type wafers, with a base resistivity of ∼3 Ω cm and a thickness of 180 μm, were textured using a KOH solution and rounded with a wet-chemical post-treatment. As cleaning steps, the samples received a subsequential pre-treatment comprising Radio Corporation of America (RCA) 1 and 2, and nitric acid oxidation of silicon (NAOS) solutions. Subsequently, the wafers were dipped in a 1% diluted HF bath prior to the formation of ultra-thin oxide in an oxidation tube using a mixture of O_2 and N_2 at 610 °C. Then, the ultra-thin n-type hydrogenated amorphous silicon [a-Si:H(n^+)] layers with a thickness of 10 or 20 nm were deposited by plasma-enhanced chemical vapor deposition (PECVD). The poly-Si(n^+) films were subsequently crystallized at 900 °C. The hydrogenation scheme of the poly-Si(n^+) contact was performed by the deposition of a sacrificial spatial atomic layer deposited (sALD) AlO_x film. The samples were annealed at 600 °C in an N_2 environment to allow hydrogen diffusion to the Si interface. Finally, the AlO_x films were etched in a 1% diluted HF bath. For contact resistance measurements [as shown in Fig. 1(d)], approximately 300 nm thick Ag films were sputtered on both sides.

The surface passivation quality of the cell precursors was measured by using a Sinton WCT-120 tool in the transient mode. Note that five measurements were taken per sample of which the average minority carrier lifetime value is reported here. An optical constant of 0.7 was used for the samples without ITO, while an optical constant of 1.05 was used for the samples with ITO to account for the anti-reflective properties of the ITO. Contact resistivity of the

03 June 2024 13:21:40

© Author(s) 2023

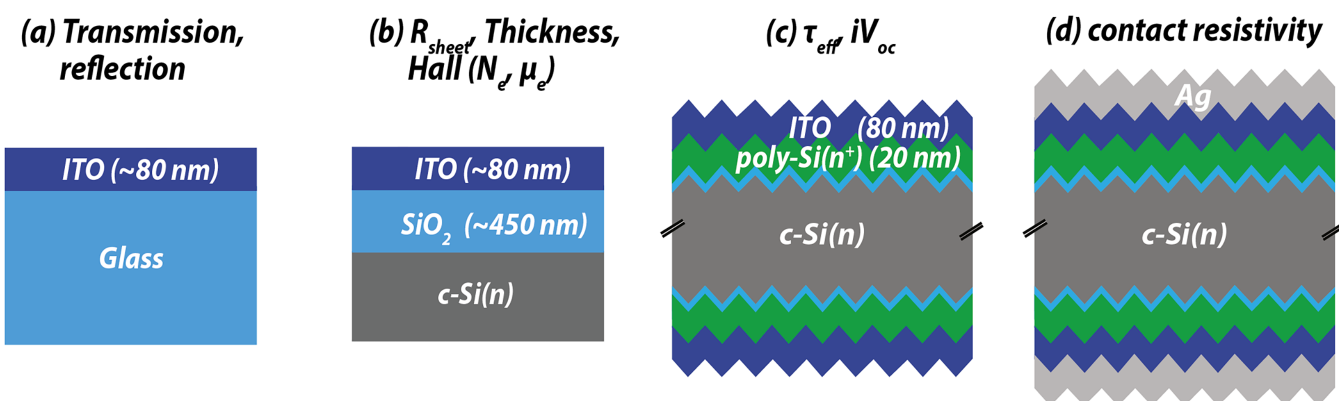

FIG. 1. Schematic overview of test measurement structures for (a) transmission and reflection, (b) Hall and R_{sheet} measurements on a thick SiO_2 substrate, (c) effective lifetime of the symmetric poly-Si(n+) contact, (d) contact resistivity measurement with Ag electrodes.

overall c-Si/SiO_x/poly-Si(n^+)/ITO/Ag stack was measured by vertical dark *IV*-measurement across the sample using the formula $R_{Total} = R_{base} + 2 \times R_{contact}$, where R_{contact} represents the overall contact resistance between the Si base material and the Ag contact.

III. RESULTS

A. Sputtering and PLD-induced damage of ITO deposition on ultra-thin poly-Si contacts

In order to compare the deposition-induced damage caused by sputtering and PLD, the effective lifetime (τ_{eff}) at an injection density of 10^{15} cm^{-3} was measured on samples with 10 and 20 nm thick poly-Si(n^+) contacts. Sputtered and PLD ITO samples were fabricated at room temperature (RT) and at a similar operating pressure of 0.01 mbar. In addition, post-annealing treatments were performed in air at 190 °C and, subsequently, at 350 °C after ITO deposition. Figure 2 shows a comparison in τ_{eff} between sputtered and PLD ITO layers deposited on 10 and 20 nm thick poly-Si(n+) contacts and at different processing stages.

The initial τ_{eff} of the sample with the 10 nm thick poly-Si contact (after hydrogenation) is lower than that with the 20 nm contact. This is caused by an unoptimized doping concentration

03 June 2024 13:21:40

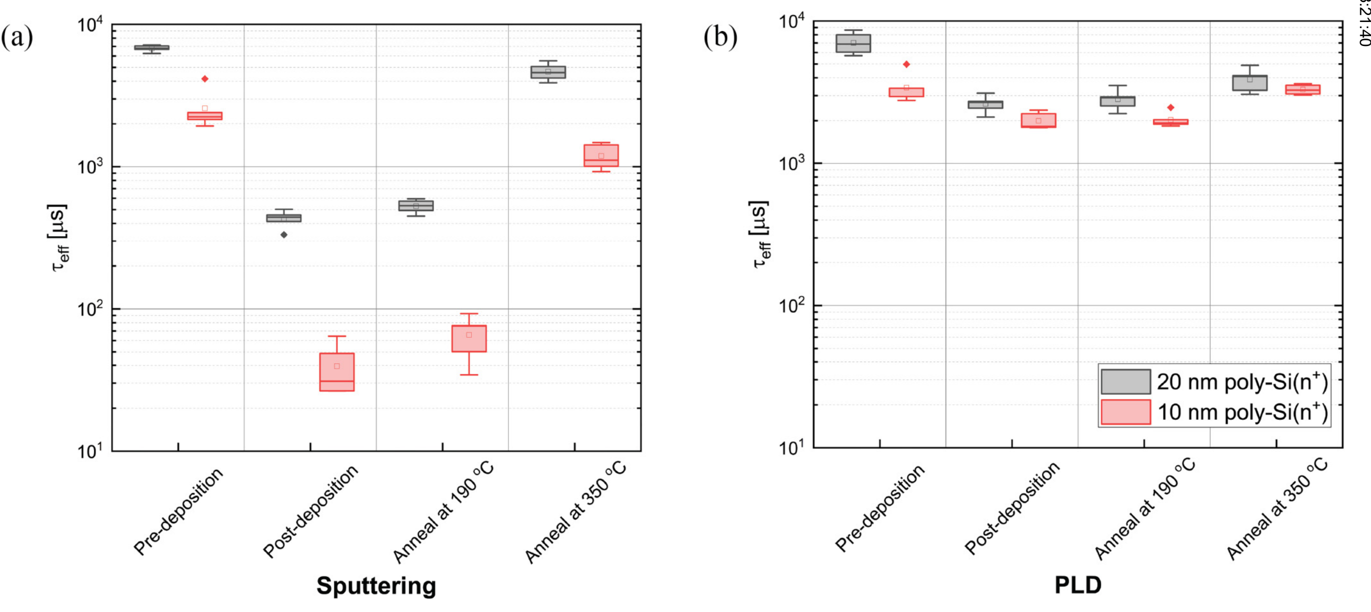

FIG. 2. Change in τ_{eff} for 10 and 20 nm poly-Si contacts before and after ITO deposition by (a) sputtering and (b) PLD, and post-annealing treatment at 190 and 350 °C. The PLD ITO layer was deposited at RT with a O_2 pressure of 0.012 mbar, a laser repetition rate of 50 Hz, and a fluence of 1.55 J/cm^2.

© Author(s) 2023

and crystallization step of the poly-Si(n^+) layer (this effect can be seen in Fig. S1 in the supplementary material), thereby resulting in the non-ideal diffusion of dopant into the c-Si substrate. Consequently, a reduced field-effect passivation is perceived by the sample with the thinner poly-Si layer. After ITO deposition by sputtering, the surface passivation quality of the sample with the 20 nm thick contact drastically decreases. Further aggravated damage is observed for the sample with the thinner layer as a drop in τ_{eff} to about 30 μs is detected. Post-deposition annealing treatment at 190 °C only slightly improves τ_{eff} for both samples with the 10 and 20 nm poly-Si thicknesses. Nevertheless, after subsequent annealing treatment at 350 °C, τ_{eff} of the 10 and 20 nm poly-Si contact samples considerably improves to around 1 and 4.6 ms, respectively, and this trend was also observed by Tutsch *et al.*[14] While a certain level of PLD-induced damage is observed on the poly-Si contact, the decrease in τ_{eff} is significantly reduced in comparison with sputtering as τ_{eff} above 2 ms is achieved for both poly-Si thicknesses. Additionally, the damage caused by PLD seems to be independent on the thickness of the poly-Si contact, as a comparable level of surface passivation is achieved directly after deposition. Likewise, annealing treatment at 190 °C results in minimal surface passivation change, while a slight lifetime improvement is perceived at 350 °C. In the case of the 20 nm poly-Si contact, the sputtered sample demonstrates a superior average τ_{eff} of 4.6 ms compared to the PLD counterpart (~3.9 ms) after annealing at 350 °C. The following part will explore the influence of laser parameters, substrate temperature (T_{sub}), and processing pressure on the deposition-induced damage corresponding to the PLD technique.

1. Influence of laser fluence and repetition rate

Laser settings can have a considerable influence on the plasma parameters and on the material of the layers deposited.[15,16] The KrF excimer laser creates ultra-short pulses in the order of ns duration where the frequency of these pulses, i.e., repetition rate, can influence the plasma interaction with the gas present in the process chamber and, subsequently, the growth mechanism. Conversely, the laser fluence of the pulses dictates the ablation properties of the target material. For instance, low and high laser fluences can result in evaporation-like deposition and sputtering-like ablation, respectively.[15]

Here, the repetition rate and laser fluence for depositing ITO were varied from 20 to 50 Hz and 0.93 to 1.55 J/cm^2, respectively, as shown in Fig. 3. The variation in the laser fluence and repetition rate shows no significant impact on the PLD-induced damage, as τ_{eff} drops from about 5–6 ms to 2 ms after deposition. This indicates that the laser process parameters do not play an important role in minimizing the damage in the range of laser settings investigated here. A sufficient thermal budget of 350 °C is required to partially recover the PLD-induced damage.

2. Effect of deposition temperature

Next, we investigate the effect of deposition temperature (T_{dep}) on the change in the surface passivation quality of our 20 nm poly-Si(n$^+$) contacts, as shown in Fig. 4. T_{dep} is varied between 20 and 400 °C, while $P_{chamber}$ and the $O_2/(O_2 + Ar)$ flow ratio are maintained at 0.02 mbar and 0.2, respectively. The change in surface passivation after subsequent ITO deposition and annealing at 190 and 350 °C shows similar trends as previously observed for T_{dep} between 20 and 200 °C. However, at T_{dep} = 400 °C, the surface

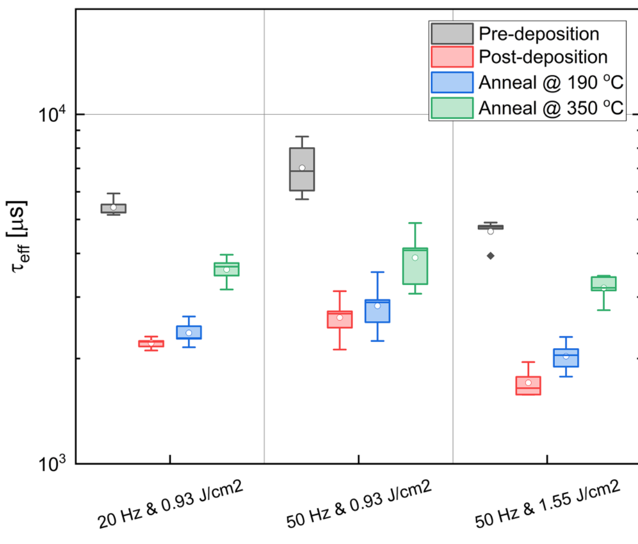

FIG. 3. Influence of the laser repetition rate and fluence on the τ_{eff} of 20 nm poly-Si contacts. ITO films are deposited at RT, with $P_{chamber}$ = 0.02 mbar, and O_2 to Ar ratio = 0.2.

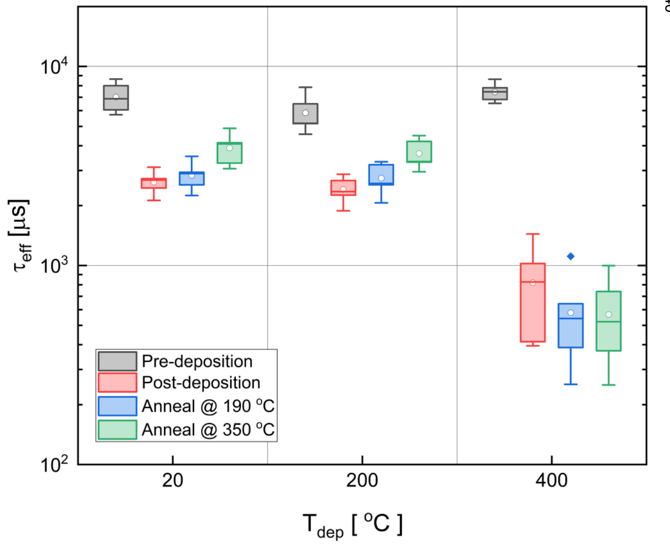

FIG. 4. Effect of T_{dep} (20–400 °C) on the surface passivation of 20 nm poly-Si contacts. ITO films are deposited at a $P_{chamber}$ = 0.02 mbar, O_2 to O_2 + Ar ratio = 0.2, repetition rate = 50 Hz, and laser fluence = 0.93 J/cm^2.

03 June 2024 13:21:40

© Author(s) 2023

passivation quality after ITO deposition is further reduced and no recovery is observed after subsequent anneals. This could be due to the effusion of hydrogen, which occurs during deposition at higher temperature and at low pressure and, thereby, leaves the dangling bonds at the Si interface unpassivated.

3. Effect of chamber pressure

Last, the effect of the chamber pressure ($P_{chamber}$) on the induced damage is investigated. Figure 5 shows the change in surface passivation quality with respect to the varying $P_{chamber}$ from 0.02 to 0.2 mbar. Note that the initial surface passivation of the 20 nm poly-Si contact samples for the different process chamber pressures is slightly different. After ITO deposition at $P_{chamber} = 0.1$ mbar, a similar relative drop in τ_{eff} is observed to poly-Si contacts with ITO deposited at 0.02 mbar. However, a notable increase in τ_{eff} is observed after annealing at 190 °C and it slightly increases after subsequent annealing treatment at 350 °C. At $P_{chamber} = 0.2$ mbar, the drop in τ_{eff} is less while no change in τ_{eff} is perceived after annealing, not even for the samples annealed at 350 °C. This is indicative that the PLD-induced damage is less for ITO layers deposited at higher pressure and corresponding to the level that is observed after recovery anneals.

IV. CONTACT RESISTIVITY

In this section, the influence of PLD parameters on the contact resistivity of overall 20 nm poly-Si contacts is investigated. Figure 6 shows the overall contact resistivity of c-Si/poly-Si(n^+)/ITO/Ag structures, meaning the overall $R_{contact}$ from the base to metal, with a reference sputtered and PLD ITO films deposited under varying T_{dep} (20, 200 °C) and $P_{chamber}$ (0.012–0.1 mbar) conditions. These contacts were subsequently annealed at temperatures between 190 and 350 °C in air. Note that the PLD ITO film was deposited at 0.1 mbar and 200 °C, since higher deposition pressure and lower deposition temperature resulted in poor layer conductivity. Additionally, an oxygen pressure of 0.012 mbar (no Ar gas) was selected to deposit ITO, because optimal opto-electrical properties were obtained (as observed in Fig. 7) at this pressure while no difference in surface passivation was observed with ITO deposited at 0.02 mbar.

The Ag/poly-Si(n^+)/SiO_x/c-Si(n) contact without an ITO film displays a low contact resistivity of 20 mΩ cm^2. This means that the main contribution of the contact resistivity in a complete structure can be attributed to the poly-Si/ITO interface. In order to minimize the impact of series resistance on fill factor losses, contact resistivity below 100 mΩ cm^2 should be achieved.[17] As-deposited poly-Si contacts with PLD ITO layers show contact resistivities below 100 mΩ cm^2. In comparison, the poly-Si contact with sputtered ITO shows a contact resistivity of about 300 mΩ cm^2. The higher contact resistivity of our reference sputtered ITO structure could be due to the lower carrier concentration of the sputtered ITO, which impedes the transport of majority carriers (reduction in barrier width).[18] A significant increase in the contact resistivity is observed for our sputtering reference for annealing temperature above 250 °C. Similar behavior is observed for a poly-Si contact with a PLD ITO layer deposited at 0.1 mbar where a steep increase in the contact resistivity is noticed at annealing temperature of 350 °C. On the other hand, contacts with PLD ITO layers deposited at low pressures are thermally more stable even after a subsequential anneal at 350 °C.

03 June 2024 13:21:40

FIG. 5. Effect of $P_{chamber}$ (0.02–0.2 mbar) on the surface passivation of 20 nm poly-Si contacts. ITO films are deposited at RT with $O_2/O_2 + Ar$ ratio = 0.2, repetition rate = 50 Hz, and laser fluence = 0.93 J/cm^2.

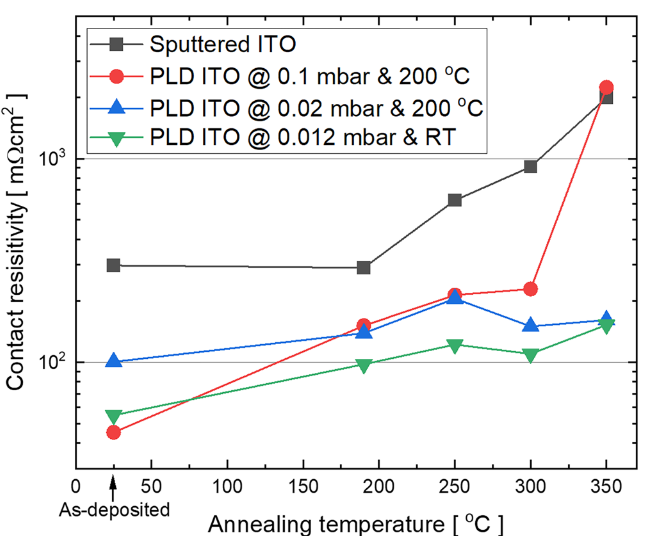

FIG. 6. Overall contact resistivity of 20 nm thick poly-Si contacts with sputtered and PLD ITO layers cumulatively annealed from 190 to 350 °C for 5 min at each annealing temperature. PLD ITO deposited at 0.1 mbar has an $O_2/Ar + O_2$ ratio of 0.1, a laser repetition rate of 50 Hz, and a laser fluence of 1.55 J/cm^2.

© Author(s) 2023

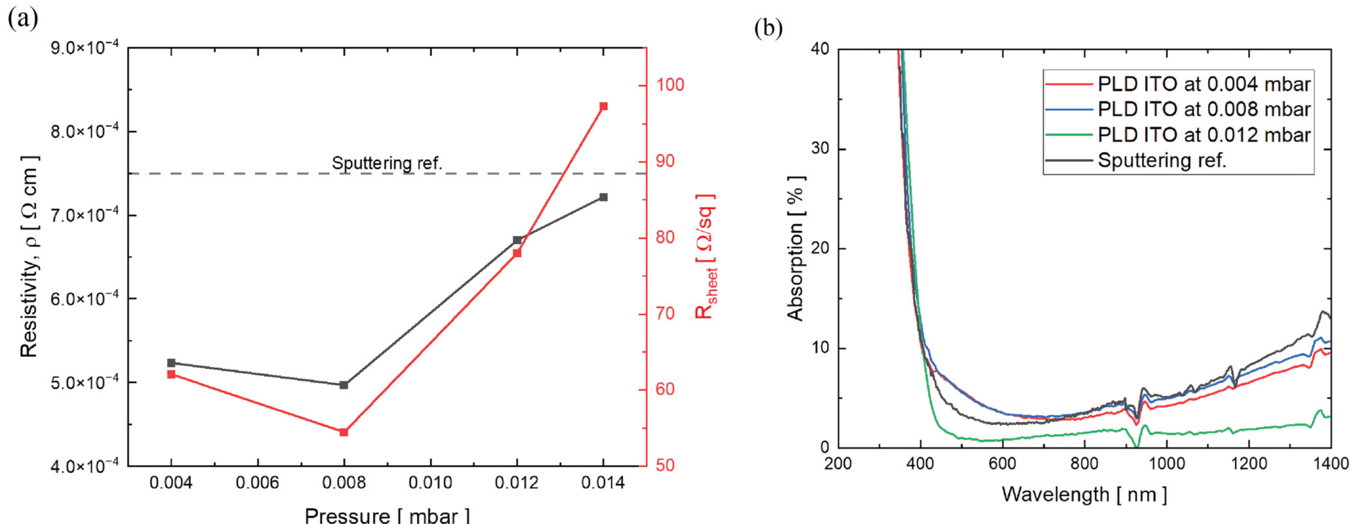

FIG. 7. Resistivity and R_{sheet} at varying oxygen pressures (0.004–0.014 mbar) (a) and absorption spectrum (b) of PLD ITO films. Opto-electrical properties of sputtered ITO reference are also included.

V. OPTO-ELECTRICAL PROPERTIES OF PLD ITO LAYERS

The effect of PLD parameters on the ITO opto-electrical properties is discussed in this section. 80 nm thick ITO films were deposited at RT with varying total oxygen pressures between 0.004 and 0.014 mbar. The laser fluence and repetition rate are kept at 0.93 J/cm^2 and 50 Hz, respectively. Figures 7(a) and 7(b) show ρ and R_{sheet}, and the absorption (dependent on the wavelength) of the deposited ITO layers, respectively. The sputtering reference results in a ρ of 0.75 mΩ cm after an annealing treatment at 190 °C. For PLD ITO films, a minimum resistivity of 0.49 mΩ cm^2 is obtained at a chamber pressure of 0.008 mbar and increases at higher pressure. While a minimum resistivity can be obtained at a total oxygen pressure of 0.008 mbar, the absorption of the ITO film in the visible and infrared region is relatively high in comparison with the ITO layer deposited at 0.012 mbar. For a better trade-off between resistivity and absorption, the ITO layer deposited at 0.012 mbar is selected for further development.

Figure 8(a) shows the ITO thickness dependence on the repetition rate for the laser fluence of 0.93 and 1.55 J/cm^2. An increase in the repetition rate and laser fluence results in a thicker layer since more material will be ablated at higher laser fluence and at higher repetition rates. Figures 8(b) and 8(c) show the mobility (μ_e) and carrier concentration (N_e) of the ITO layers with respect to the repetition rate, respectively, for laser fluences of 0.93 and 1.55 J/cm^2. The ITO layers are also subjected to annealing treatment in air at 190 °C for 30 min. Prior to the thermal treatment, for the as-deposited ITO layers, a higher laser fluence results in an increase in μ_e. The μ_e of ITO layers do not show a strong dependence on the repetition rate. After annealing, the μ_e of all ITO layers show an increase. For a higher repetition rate, a slight decrease is observed for the lower fluence, while for a higher fluence, no dependence on the repetition rate is observed. The increase in μ_e is most likely caused by an increase in the grain size in the polycrystalline ITO layers.[19] The μ_e of ITO layers deposited at a fluence of 1.55 J/cm^2 shows minimal dependence on the repetition rate. As-deposited ITO layers show a high N_e independent of the laser fluence. After annealing, the N_e of the ITO layers decreases considerably and depends on the repetition rate; for both laser fluences, an increase in N_e is observed for higher repetition rates.

VI. DISCUSSION

Significant induced damage resulting from ITO deposition is evident on ultra-thin poly-Si contact structures. Various factors, including work function mismatch between the contact layers, high-energy species, and radiation emitted during deposition, can contribute to the reduction in the surface passivation of these contacts. A work function mismatch between the poly-Si(n^+) and the ITO layers leads to a reduction in field-effect passivation, particularly noticeable at low injection levels.[20] This phenomenon is particularly observed in a-Si:H(p^+) contacts and can be attributed to their comparatively lower doping efficiency when compared to their n-type counterparts.[18,21] However, it is unlikely that the work function mismatch between the poly-Si(n^+) and the ITO layer significantly influences the passivation quality of our 20 nm poly-Si(n+) contact. This assertion is supported by the absence of substantial improvement in the charge carrier lifetime after etching off the ITO layer (refer to Fig. S2 in the supplementary material).

Conversely, it is difficult to completely disentangle the different effects caused by plasma radiation, electrons, x rays (arising from ions or electrons), and high energy particles bombardments. Several reports specify that the main cause of the subsequent damage is related to high energetic species that bombard the poly-Si contact.[14,18,22,23] This is because sputtering relies on the

03 June 2024 13:21:40

© Author(s) 2023

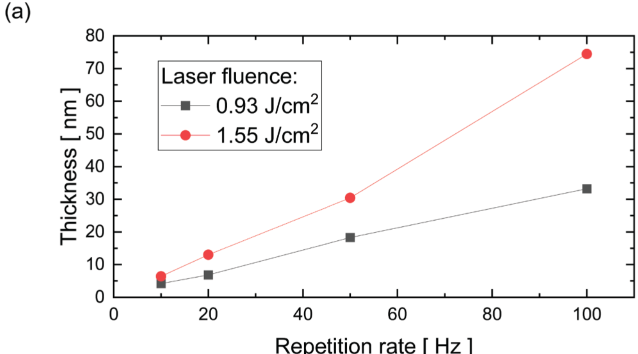

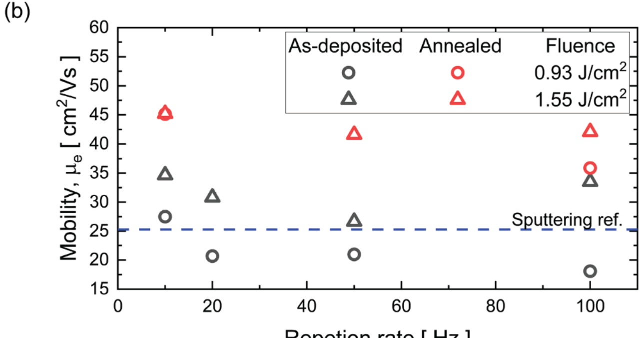

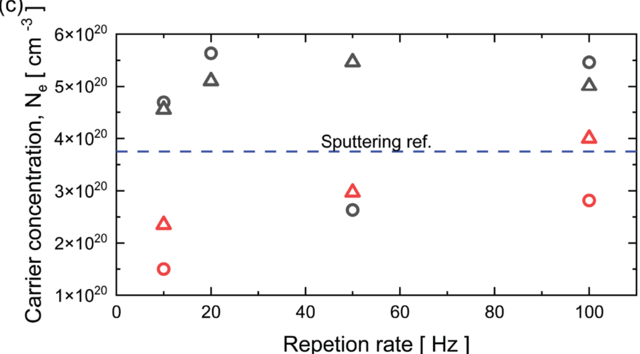

FIG. 8. Effect of PLD variations on (a) the ITO layer thickness, (b) mobility, and (c) carrier concentration properties of the deposited ITO layer. Electrical properties of the sputtered ITO reference are also included.

ejection of the bulk target material to the substrate by momentum transfer; high energetic ions formed by the plasma (typically Ar ions) bombard the target, which results in the ejection of the target material.[24] Consequently, several high energetic species are formed at the target surface (O^- and In^- from ITO target) and in the plasma, and are accelerated toward the substrate by a potential difference between the target and the substrate. These high energy ions and species often have sufficient kinetic energy to penetrate through several nanometers of Si, thereby rupturing bonds present at and near the Si/SiO_x interface. For plasma radiation induced damage, Tutsch *et al.*[14] showed that almost no degradation of 10 nm poly-Si based contact stacks was observed for photon with energy below 4 eV. However, the higher energy photons (~9 eV), originating from argon and oxygen plasmas, could cause significant structural damage to poly-Si contacts. For instance, Profijt *et al.*[25] showed that high energy ultraviolet photons in vacuum can cause significant loss in surface passivation on the Si substrate with deposited Al_2O_3 films. While the thickness of the poly-Si(n^+) plays an important role in shielding the damage caused by the ion bombardment, significant interface defects are still created at the Si/SiO_x interface for a 20 nm thick poly-Si layer. Several strategies exist to mitigate the damage caused by sputtering, such as increasing the deposition pressure and lowering the deposition power.[26] However, these processing conditions can result in ignition issues, while high pressure can be problematic for obtaining a high-quality layer.[27]

On the contrary, the induced damage caused by the PLD technique is considerably reduced in comparison with our sputtering reference. This can be ascribed to the physical differences in deposition techniques, for PLD ablation of the target material is prompted by laser light absorption while sputtering relies on Ar ion bombardment. In PLD, a plasma plume is formed during the ablation process and is allowed to expand in the background gas due to the high-pressure gradients in the initial part of the plume.[28–30] The plume is allowed to slow down in the background gas and the atoms eventually diffuse out of the plume and migrate to the substrate.[31] For ultra-thin poly-Si(n^+) based contacts, the "softer" deposition properties of PLD result in superior surface passivation properties after ITO deposition. Furthermore, this behavior is also apparent on 10 nm poly-Si contacts, which shows a minor degradation in surface passivation quality, unlike sputtering-induced damage. Nevertheless, the deposition of ITO on poly-Si(n^+) layers by PLD still results in a certain level of damage. This induced damage is not related to the fluence (ranging between 0.93 and 1.55 J/cm^2) and the repetition rate of the laser. A high chamber pressure is beneficial to mitigate the damage due to the thermalization of harmful species, hence resulting in a softer deposition on the poly-Si contact. Similar effects were observed on a buffer-free semi-transparent perovskite solar cell where an increase in the pressure resulted in damage-free deposition.[12] While PLD-induced damage caused by the plasma formation is present, the plasma formed by PLD is very complex and requires further investigations to determine the root cause of the PLD-induced damage. Possible causes, such as high energy photons and soft x rays—arising from ion or electron bombardment—should not be excluded.[32,33]

Although the root causes of the induced-deposition damage are not completely clarified, the surface passivation of the poly-Si contact can be almost completely repaired by post-deposition annealing treatment at 350 °C. The change in surface passivation quality after annealing is mainly attributed to the modification of the chemical passivation quality since a change in carrier population in the contact is unlikely due to the relatively low thermal budget; a thermal budget of 700–1050 °C is typically required to cause a change in poly-Si crystallization and dopant activation and diffusion. The surface passivation recovery of poly-Si based contacts is often reported after a post-deposition thermal annealing treatment at temperatures around 350 °, which also corresponds to our findings. This temperature requirement matches with the activation

03 June 2024 13:21:40

© Author(s) 2023

energy required for effective hydrogenation of poly-Si contacts. For instance, hydrogen plasma exposure or hydrogen-rich capping layers often require a processing temperature higher than 300 °C to allow for effective diffusion of hydrogen to the SiO_x interface.[34] It is highly plausible that the H atoms, in the vicinity of the SiO_x/c-Si interface, are allowed to diffuse again to the interface upon post-deposition annealing and, thereby, passivate the Si dangling bonds present at the surface, thus improving the chemical passivation quality.

The overall contact resistivity of the poly-Si based contact with a sputtered ITO layer shows a significant increase at annealing temperatures higher than 250 °C. Various works[14,18,20,21] show similar trends, and this is commonly linked to the formation of a parasitic SiO_x interlayer at the poly-Si/ITO interface.[18] This interlayer is allowed to grow rapidly under increasing thermal budget, which, in turn, results in an inefficient tunneling transport of majority carriers to the ITO layer. Although annealing at 350 °C is required to recover the sputtering-induced damage of our poly-Si contact, the high contact resistivity results in an inefficient transport of majority carriers. Contacts with PLD ITO deposited at 200 °C show good contact resistivity, while a slight increase is observed with annealing temperature. However, the significant increase in the contact resistivity for contacts with PLD ITO deposited at high pressure suggests that the high partial O_2 pressure deposition promotes the formation of a parasitic oxide at the ITO/poly-Si(n^+) interface. Nevertheless, due to the thermalization of harmful species at high pressure, annealing at 190 °C is sufficient to repair the induced damage at chamber pressures higher than 0.1 mbar. PLD ITO deposited at room temperature and low pressure enables low contact resistivity and does not promote a significant increase in the contact resistivity, which possibly indicates the absence of parasitic oxide. However, further and more detailed analysis on the presence and composition of oxide is required for better understanding.

The opto-electrical properties of the PLD deposited ITO layer shows strong dependence on the total oxygen pressure. On the other hand, an increase in the ITO deposition rate is observed with increasing repetition rate and laser fluency without majorly affecting the layer mobility after post-deposition annealing treatment at 190 °. Specifically, a remarkable ITO layer mobility of 42.1 $cm^2/V\,s$ and a carrier concentration of $4.0 \times 10^{20}\,cm^{-3}$ were attained at a repetition rate of 100 Hz and a laser fluency of 1.43 J/cm^2. Note that these measurements were carried out on a flat Si substrate, which might be slightly different a on textured poly-Si substrate, and that final layer optimization should still be performed on cell level.

Nonetheless, while PLD demonstrates significant advantages for solar cell applications, the constraint imposed by the confined laser spot size presents a substantial impediment to its implementation in high-throughput solar cell processes. Resolving this limitation requires dedicated efforts aimed at expanding the scalability of PLD techniques to large area substrates. Despite this challenge, PLD has exhibited significant benefits on perovskite solar cells, as significant work has been done on all active layers of the solar cell.[12,35,36] This progress is particularly promising for the integration of perovskite solar cells into tandem structures. Such advancements can pave the way for the seamless integration of perovskite solar cells with silicon-based tandem solar cells, offering an attractive avenue for elevating the efficiency and overall performance of the next generation of solar cell technologies.

VII. CONCLUSIONS

Reducing the thickness of the poly-Si layer is essential to mitigate the parasitic absorption losses caused by the contact. However, this, in case ITO is applied by sputtering, aggravates the sputtering-induced damage on poly-Si layers thinner than 20 nm. Although post-deposition annealing treatment can be performed to partially recover the damage, the contact resistivity drastically increases. Alternatively, TCO deposition by PLD has shown to be beneficial in minimizing the damage at the Si/SiO_x interface while maintaining low contact resistivity even after post-deposition annealing at 350 °C. Furthermore, the damage originating from PLD is not thickness dependent, which allows for the development of thinner poly-Si contacts.

SUPPLEMENTARY MATERIAL

See the supplementary material for the determination of poly-Si(n^+) doping profiles.

ACKNOWLEDGMENTS

The authors would like to thank Martin Koppes, Eelko Hoek, and Benjamin Kikkert for the fabrication of the poly-Si(n^+) sample. This work was financially supported by Top consortia for Knowledge and Innovation (TKI) Solar Energy programs "COMPASS" (TEID215022), "RADAR" (TEUE116905), and MOMENTUM (TKI Energy PPS Toeslag Project No. 1821101) of the Ministry of Economic Affairs of The Netherlands.

03 June 2024 13:21:40

AUTHOR DECLARATIONS

Conflict of interest

The authors have no conflicts to disclose.

Author Contributions

Mike Tang Soo Kiong Ah Sen: Conceptualization (equal); Data curation (equal); Formal analysis (equal); Investigation (equal); Methodology (equal); Supervision (equal); Writing – original draft (equal); Writing – review & editing (equal). **Agnes Mewe:** Funding acquisition (equal); Methodology (equal); Project administration (equal); Supervision (equal); Writing – review & editing (equal). **Jimmy Melskens:** Conceptualization (equal); Data curation (equal); Formal analysis (equal); Investigation (equal); Methodology (equal); Supervision (equal); Writing – review & editing (equal). **Jons Bolding:** Conceptualization (equal); Data curation (equal); Investigation (equal); Methodology (equal); Writing – original draft (equal). **Mike van de Poll:** Data curation (equal); Methodology (equal); Writing – review & editing (equal). **Arthur Weeber:** Funding acquisition (equal); Project administration (equal); Supervision (equal); Writing – review & editing (equal).

© Author(s) 2023

DATA AVAILABILITY

The data that support the findings of this study are available from the corresponding author upon reasonable request.

REFERENCES

[1] V. Shaw, "Chinese PV Industry Brief: JinkoSolar achieves 26.4% efficiency for n-type TOPCon solar cell," URL: https://www.pv-magazine.com/2022/12/09/chinese-pv-industry-brief-jinkosolar-achieves-26-1-efficiency-for-n-type-topcon-solar-cell/ (last accessed on 12/23/2022).

[2] C. N. Kruse, S. Schäfer, F. Haase, V. Mertens, H. Schulte-Huxel, B. Lim, B. Min, T. Dullweber, R. Peibst, and R. Brendel, "Simulation-based roadmap for the integration of poly-silicon on oxide contacts into screen-printed crystalline silicon solar cells," Sci. Rep. **11**(1), 1–14 (2021).

[3] R. Street, D. Biegelsen, and J. Stuke, "Defects in bombarded amorphous silicon," Philos. Mag. B **40**(6), 451–464 (1979).

[4] B. Demaurex, S. De Wolf, A. Descoeudres, Z. C. Holman, and C. Ballif, "Damage at hydrogenated amorphous/crystalline silicon interfaces by indium tin oxide overlayer sputtering," Appl. Phys. Lett. **101**(17), 171604 (2012).

[5] T. F. Wietler, B. Min, S. Reiter, Y. Larionova, R. Reineke-Koch, F. Heinemeyer, R. Brendel, A. Feldhoff, J. Krugener, D. Tetzlaff, and R. Peibst, "High temperature annealing of ZnO:Al on passivating POLO junctions: Impact on transparency, conductivity, junction passivation, and interface stability," IEEE J. Photovolt. **9**(1), 89–96 (2019).

[6] L. Tutsch, F. Feldmann, M. Bivour, W. Wolke, M. Hermle, and J. Rentsch, "Integrating transparent conductive oxides to improve the infrared response of silicon solar cells with passivating rear contacts," AIP Conf. Proc. **1999**, 040023 (2018).

[7] M. Wimmer, M. Bär, D. Gerlach, R. G. Wilks, S. Scherf, C. Lupulescu, F. Ruske, R. Félix, J. Hüpkes, G. Gavrila, M. Gorgoi, K. Lips, W. Eberhardt, and B. Rech, "Hard x-ray photoelectron spectroscopy study of the buried Si/ZnO thin-film solar cell interface: Direct evidence for the formation of Si-O at the expense of Zn-O bonds," Appl. Phys. Lett. **99**(15), 152104 (2011).

[8] C. Messmer, M. Bivour, C. Luderer, L. Tutsch, J. Schon, and M. Hermle, "Influence of interfacial oxides at TCO/doped Si thin film contacts on the charge carrier transport of passivating contacts," IEEE J. Photovolt. **10**(2), 1–8 (2019).

[9] L. Tutsch, F. Feldmann, B. MacCo, M. Bivour, E. Kessels, and M. Hermle, "Improved passivation of n-type poly-Si based passivating contacts by the application of hydrogen-rich transparent conductive oxides," IEEE J. Photovolt. **10**(4), 986–991 (2020).

[10] J. M. Dekkers and J. A. Janssens, "Method for depositing a target material onto a organic electrically functional material," US Patent 10,128,467. Nov. 2018.

[11] S. Schubert, F. Schmidt, H. Von Wenckstern, M. Grundmann, K. Leo, L. Müller-Meskamp, "Eclipse pulsed laser deposition for damage-free preparation of transparent ZnO electrodes on top of organic solar cells," Adv. Funct. Mater. **25**(27), 4321–4327 (2015).

[12] Y. Smirnov, L. Schmengler, R. Kuik, P.-A. Repecaud, M. Najafi, D. Zhang, M. Theelen, E. Aydin, S. Veenstra, S. De Wolf, and M. Morales-Masis, "Scalable pulsed laser deposition of transparent rear electrode for perovskite solar cells," Adv. Mater. Technol. **6**(2), 2000856 (2021).

[13] Y. Smirnov, P. A. Repecaud, L. Tutsch, I. Florea, K. P. S. Zanoni, A. Paliwal, H. J. Bolink, P. R. Cabarrocas, M. Bivour, and M. Morales-Masis, "Wafer-scale pulsed laser deposition of ITO for solar cells: Reduced damage vs. interfacial resistance," Mater. Adv. **3**(8), 3469–3478 (2022).

[14] L. Tutsch, F. Feldmann, J. Polzin, C. Luderer, M. Bivour, A. Moldovan, J. Rentsch, and M. Hermle, "Implementing transparent conducting oxides by DC sputtering on ultrathin SiO_x/poly-Si passivating contacts," Sol. Energy Mater. Sol. Cells **200**, 109960 (2019).

[15] J. Schou, "Physical aspects of the pulsed laser deposition technique: The stoichiometric transfer of material from target to film," Appl. Surf. Sci. **255**(10), 5191–5198 (2009).

[16] A. Ojeda-G-P, M. Döbeli, and T. Lippert, "Influence of plume properties on thin film composition in pulsed laser deposition," Adv. Mater. Interfaces **5**(18), 1701062 (2018).

[17] J. Melskens, B. W. H. Van De Loo, B. Macco, L. E. Black, S. Smit, and W. M. M. Kessels, "Passivating contacts for crystalline silicon solar cells: From concepts and materials to prospects," IEEE J. Photovolt. **8**(2), 373–388 (2018).

[18] C. Messmer, M. Bivour, C. Luderer, L. Tutsch, J. Schon, and M. Hermle, "Influence of interfacial oxides at TCO/doped Si thin film contacts on the charge carrier transport of passivating contacts," IEEE J. Photovolt. **10**(2), 343–350 (2020).

[19] B. Macco, H. C. M. Knoops, and W. M. M. Kessels, "Electron scattering and doping mechanisms in solid-phase-crystallized In_2O_3:H prepared by atomic layer deposition," ACS Appl. Mater. Interfaces **7**(30), 16723–16729 (2015).

[20] R. Rößler, C. Leendertz, L. Korte, N. Mingirulli, B. Rech, R. Rößler, C. Leendertz, L. Korte, N. Mingirulli, and B. Rech, "Impact of the transparent conductive oxide work function on injection-dependent a-Si:H/c-Si band bending and solar cell parameters," J. Appl. Phys. **113**(14), 144513 (2013).

[21] W. E. Spear and P. G. Le Comber, "Substitutional doping of amorphous silicon," Solid State Commun. **17**(9), 1193–1196 (1975).

[22] L. Tutsch, F. Feldmann, M. Bivour, W. Wolke, M. Hermle, and J. Rentsch, "Integrating transparent conductive oxides to improve the infrared response of silicon solar cells with passivating rear contacts," AIP Conf. Proc. **1999**, 40018 (1999).

[23] Y. Larionova, H. Schulte-Huxel, B. Min, S. Schäfer, T. Kluge, H. Mehlich, R. Brendel, and R. Peibst, "Ultra-thin poly-Si layers: Passivation quality, utilization of charge carriers generated in the poly-Si and application on screen-printed double-side contacted polycrystalline Si on oxide cells," Sol. RRL **4**(10), 2000177 (2020).

[24] E. Aydin, C. Altinkaya, Y. Smirnov, M. A. Yaqin, K. P. S. Zanoni, A. Paliwal, Y. Firdaus, T. G. Allen, T. D. Anthopoulos, H. J. Bolink, M. Morales-Masis, and S. D. Wolf, "Sputtered transparent electrodes for optoelectronic devices: Induced damage and mitigation strategies," Matter **4**(11), 3549–3584 (2021).

[25] H. B. Profijt, P. Kudlacek, M. C. M. van de Sanden, and W. M. M. Kessels, "Ion and photon surface interaction during remote plasma ALD of metal oxides," J. Electrochem. Soc. **158**(4), G88 (2011).

[26] M. Köhler, M. Pomaska, P. Procel, R. Santbergen, A. Zamchiy, B. Macco, A. Lambertz, W. Duan, P. Cao, B. Klingebiel, S. Li, A. Eberst, M. Luysberg, K. Qiu, O. Isabella, F. Finger, T. Kirchartz, U. Rau, and K. Ding, "A silicon carbide-based highly transparent passivating contact for crystalline silicon solar cells approaching efficiencies of 24%," Nat. Energy **6**(5), 529–537 (2021).

[27] A. J. Bett, K. M. Winkler, M. Bivour, L. Cojocaru, Ö Kabakli, P. S. C. Schulze, G. Siefer, L. Tutsch, M. Hermle, S. W. Glunz, and J. C. Goldschmidt, "Semi-transparent perovskite solar cells with ITO directly sputtered on spiro-OMeTAD for tandem applications," ACS Appl. Mater. Interfaces **11**(49), 45796–45804 (2019).

[28] Y. Pauleau, Materials Surface Processing by Directed Energy Techniques (APS, 2006).

[29] Y. Zel'Dovich and Y. Raizer, Physics of Shock Waves and High-Temperature Hydrodynamic Phenomena (Courier Corporation, 2002).

[30] S. I. Anisimov, D. Bäuerle, and B. S. Luk'yanchuk, "Gas dynamics and film profiles in pulsed-laser deposition of materials," Phys. Rev. B **48**(16), 12076–12081 (1993).

[31] S. Amoruso, R. Bruzzese, N. Spinelli, R. Velotta, M. Vitiello, and X. Wang, "Dynamics of laser-ablated MgB_2 plasma expanding in argon probed by optical emission spectroscopy," Phys. Rev. B **67**(22), 224503 (2003).

[32] H.-U. Krebs, M. Weisheit, J. Faupel, E. Süske, T. Scharf, C. Fuhse, M. Störmer, K. Sturm, M. Seibt, H. Kijewski, D. Nelke, E. Panchenko, and M. Buback, "Pulsed laser deposition (PLD)—a versatile thin film technique," Advances in Solid State Phys. **43**, 505–518 (2003).

[33] L. Tutsch, "Implementing sputter-deposited transparent conductive metal oxides into passivating contacts for silicon solar cells," PhD dissertation (Universität Freiburg, 2020).

03 June 2024 13:21:40

© Author(s) 2023

[34]B. W. H. Van De Loo, B. Macco, J. Melskens, W. Beyer, and W. M. M. Kessels, "Silicon surface passivation by transparent conductive zinc oxide," J. Appl. Phys. **125**(10), 105305 (2019).
[35]T. Soto-Montero, S. Kralj, W. Soltanpoor, J. S. Solomon, J. S. Gomez, K. P. S. Zanoni, A. Paliwal, H. J. Bolink, C. Baeumer, A. P. M. Kentgens, and M. Morales-Masis, "Single-Source vapor-deposition of $MA_{1-x}FA_xPbI_3$ perovskite absorbers for solar cells," Adv. Funct. Mater. (published online, 2023).
[36]Q. Zhiwen, H. Gong, G. Zheng, S. Yuan, H. Zhang, X. Zhu, H. Zhou, and B. Cao, "Enhanced physical properties of pulsed laser deposited NiO films via annealing and lithium doping for improving perovskite solar cell efficiency," J. Mater. Chem. C **5**(28), 7084–7094 (2017).

03 June 2024 13:21:40

© Author(s) 2023